1-1-2022

Trade-offs among signal correlation, SNR, and number of snapshots for direction of arrival estimation using sparse arrays

Kevin Beshara-Flynn
University of Rhode Island, kbfports5@gmail.com

TRADE-OFFS AMONG SIGNAL CORRELATION, SNR, AND NUMBER OF SNAPSHOTS FOR DIRECTION OF ARRIVAL ESTIMATION USING SPARSE ARRAYS

BY

KEVIN BESHARA-FLYNN

A THESIS SUBMITTED IN PARTIAL FULFILLMENT OF THE

REQUIREMENTS FOR THE DEGREE OF

MASTER OF SCIENCE

IN

ELECTRICAL ENGINEERING

UNIVERSITY OF RHODE ISLAND

2022

MASTER OF SCIENCE THESIS

OF

KEVIN BESHARA-FLYNN

APPROVED:

Thesis Committee:

Major Professor Kaushallya Adhikari

Paolo Stegagno

Lora Van Uffelen

Ashutosh Giri

Brenton DeBoef
DEAN OF THE GRADUATE SCHOOL

UNIVERSITY OF RHODE ISLAND

2022

ABSTRACT

Arrays can be designed as a full array of sensors or a sparse array of sensors with an equivalent aperture. Reductions in cost, size, weight and power consumption are important factors to consider when designing an array of sensors. Sparse arrays can provide a reduction in these factors. It is important to observe the performance of sparse arrays in relation to full arrays to see if they are able to achieve similar performance. The ability for the full and sparse arrays of sensors to accurately estimate the direction of arrival (DOA) of plane waves impinging them is observed in this thesis. The Mean-squared error (MSE) of the DOA estimation is measured against the Creamer-Rao bound (CRB) as a benchmark for optimal performance for an unbiased estimator. We derive an optimal way to remove sensors for one signal impinging on an array by finding the minimum CRB. This method considers all the unique combinations a sparse array could be assembled for a given number of sensors and aperture.

Parameters such as number of sensors, sensor locations, signal-to-noise ratio (SNR), number of snapshots, and signal correlation affect the MSE and CRB. Through observing trends in the MSE as a result of changing these parameters we can come to conclusions to how full and sparse arrays perform as a result of adjusting these parameters. The MSE of the DOA of the full and sparse arrays is obtained through a covariance estimation from subspace-based DOA algorithms. The sample covariance and the diagonal-averaged sample covariance matrix performances are compared.

The sample covariance matrix for a full array provides the best estimations at high SNR while the diagonal-averaging method provides a more accurate estimation at low SNR. The sparse array diagonal-averaged covariance matrix estimation performs similarly to the diagonal-averaged covariance matrix of the full array, but

is still slightly worse due to missing information. How sparsity affects performance was also observed. As sparsity increases for an array, the performance change is non-linear for the MSE and CRB. Increases in signal correlation cause an increase in the overall MSE and a decrease in the overall CRB for both sparse and full arrays.

ACKNOWLEDGMENTS

I am incredibly grateful for Dr. Adhikari's guidance and support throughout the thesis process. I would also like to thank my wonderful committee members Dr. Stegagno, Dr. Van Uffelen and Dr. Giri for being part of my thesis committee. I would also like to thank M.D. Shohel Amin and Daniel Sartori for their advice as I progressed through the thesis. Lastly, I would like to thank the Office of Naval Research for funding this work.

PREFACE

This thesis was written in manuscript format and will be published in the IEEE Xplore® digital library. It was funded by the U.S. Office of Naval Research under Grant N00014-20-1-2820.

TABLE OF CONTENTS

LIST OF FIGURES

Manuscript 1

"Effects of Signal and Array Parameters on MSE and CRB in DOA Estimation"

Authors: Kevin Beshara-Flynn, Kaushallya Adhikari

Prepared for submission to the IEEE Xplore® digital library

Department of Electrical, Computer and Biomedical Engineering, University of Rhode Island, Kingston, Rhode Island, 02881, United States

MANUSCRIPT 1

1.1 Abstract

Fully populated and sparse sensor arrays are used in estimation of directions of arrival (DOAs) of plane waves arriving on the sensor arrays. Mean-squared error (MSE) in DOA estimation is compared against the Cramer-Rao bound (CRB) to test the accuracy and evaluated the performance of the estimation algorithms. For the case of one plane wave impinging on a sensor array, we derive an analytical method to find the sparse array that has the minimum CRB among all sparse arrays with an equal number of sensors and aperture.

The CRB and MSE depend on the parameters such as number of sensors, sensor locations, signal-to-noise ratio, number of snapshots, and signal covariance. Moreover, the MSE also depends on the estimation algorithm. We analyze the MSE trends of full and sparse arrays when using different covariance matrix estimates in subspace-based DOA estimation algorithms. For a full array, using a sample covariance matrix yields more accurate results at high SNR while using a diagonal-averaged covariance matrix leads to lower MSEs at low SNR. The MSE trend of a sparse array for MUSIC or MNM is similar to the MSE pattern of a full array using a diagonal-averaged covariance matrix. An analysis of the variation of MSEs with the array sparsity reveals the non-linear dependence of the CRB and MSE on the number of sensors in a sparse array.

1.2 Introduction

When a plane wave impinges on an array of sensors, the data sampled by the sensors can be used to estimate the DOA (direction of arrival) of the plane wave. DOA estimation of plane waves finds applications in many areas including sonar and radar fields. Sensor arrays that have an average intersensor spacing of more

than half the wavelength of the impinging plane waves are called *sparse arrays*. Sensor arrays that have an average intersensor spacing equal to half the wavelength are called *full arrays*. A comprehensive list of DOA estimation algorithms and their description are found in [1, 2]. Several conventional beamforming based algorithms that are applicable to both sparse and full arrays have been studied in [3, 4, 5, 6, 7, 8, 9, 10, 11, 12]. Subspace-based superresolution algorithms have also been compared for sparse and full arrays [1, 13, 14, 15, 16, 17, 18, 19]. This work focuses on two popular subspace-based algorithms: MUSIC (Multiple Signal Classification) [20] and MNM (Minimum-Norm Method) [21].

Sparse arrays have been widely studied in the context of signal detection and estimation [5, 6, 7, 8, 10, 11, 12, 1, 13, 14, 15, 16, 17, 18, 19, 2, 22, 23, 24, 25, 26, 27, 28, 29]. Most of the design criteria of these sparse arrays have been narrow mainlobe width, low peak sidelobe height, small sidelobe area, or hole-free coarrays [6, 7, 14, 22, 23, 24, 29]. An analytical method to design sparse arrays that maximize detection of known signals in Gaussian noise has been introduced [28]. Although arrays with narrow mainlobe width, low peak sidelobe height, small sidelobe area, or hole-free coarrays provide more accurate estimates of DOAs than their counterparts, these arrays do not guarantee optimality in DOA estimation. The CRB (Cramer-Rao bound) provides a benchmark against which the performances of estimation algorithms can be compared [30, 1]. For any unbiased estimator, the CRB provides a lower bound on the variance of the estimate. Thus, having an MSE (mean-squared error) that is equal to the CRB or is close to the CRB is a desired feature in DOA estimation. Thus, in this work, we derive an analytical method to design a sparse array that has the minimum CRB among all sparse arrays with an equal aperture and number of sensors. This method is for estimating the DOA of a single plane wave in white Gaussian noise.

The factors that affect the CRB and MSE include SNR (signal-to-noise ratio), number of snapshots, number of sensors in the array, sensor locations, and signal correlation. Additionally, the MSE also depends on the estimation algorithm. For two widely used subspace-based algorithms, MUSIC and MNM, this work examines the behavior of the CRB and MSE for a scenario with two closely located plane waves in white Gaussian noise. We analyze the effects of using different covariance matrix estimates, compare the MSE patterns of full and sparse arrays, and investigate the variation of the MSE with array sparsity.

Section 1.3 describes the signal model and covariance matrices. Section 1.4 introduces an analytical method for optimal sensor selection when estimating the DOA of a plane wave. Section 1.5 analyzes the MSEs of full and sparse arrays for the MUSIC and MNM algoriths. Section 1.6 summarizes the work.

Conventions: Boldface lowercase symbols represent vectors while boldface uppercase symbols represent matrices. ^{H} denotes the Hermitian operation. $\mathbf{x} \sim \mathcal{CN}(\boldsymbol{\mu}, \boldsymbol{C})$ indicates that $\mathbf{x}$ is a random vector with a complex Gaussian distribution and its mean and covariance are $\boldsymbol{\mu}$ and $\mathbf{C}$, respectively. $x \sim \mathcal{U}(-1, 1)$ indicates that x is a random variable with a uniform distribution in the range $[-1, 1]$. $\mathbf{I}_L$ denotes an $L \times L$ identity matrix. $\odot$ represents the Hadamard (element-wise) product. $E\{x\}$ represents the expected value of x. $\mathrm{Re}\{x\}$ denotes the real part of x.

1.3 Received Signal Model

Consider a linear array oriented along the positive z-axis. The sensors are on a uniform grid with $\lambda/2$ spacing where λ is the wavelength of the plane waves that are expected to impinge on the array. Fig. 1 depicts such an array where the sensor locations along the z-axis have been divided by $\lambda/2$. The filled green circles represent the sensors and filled black circles indicate missing sensors. We denote

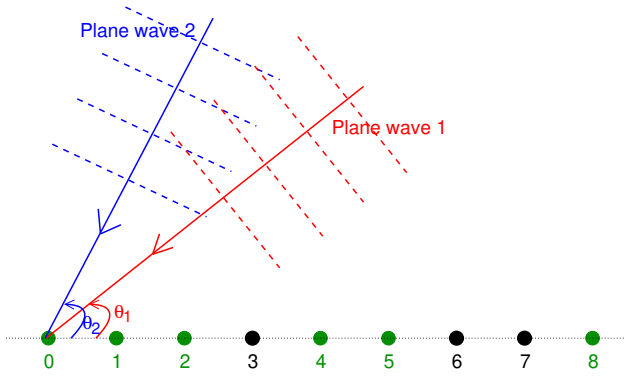

Figure 1. Two plane waves impinging on a linear array with sensors at $z = 0$, $\lambda/2$, λ, 2λ, $5\lambda/2$, 4λ.

the sensor location indicator vector for an array as $\boldsymbol{\iota}$. The n^{th} element of $\boldsymbol{\iota}$ is 1 if the array has a sensor at $n\lambda/2$ and 0 if the array does not have a sensor at $n\lambda/2$. The size of $\boldsymbol{\iota}$ is $L \times 1$, where $(L-1)\lambda/2$ is the array aperture. For the array in Fig. 1,

$$\boldsymbol{\iota} = \begin{bmatrix} 1 & 1 & 1 & 0 & 1 & 1 & 0 & 0 & 1 \end{bmatrix}^T. \tag{1}$$

The $\boldsymbol{\iota}$ for a full array with L sensors is an $L \times 1$ vector of all ones.

We define the sensor location indicator function as $\iota[l]$ for $l = 0, 1, \ldots, L-1$, where $\iota[l]$ is equal to the l^{th} element of $\boldsymbol{\iota}$. The coarray corresponding to the sensor location indicator function $\iota[l]$ is defined as [1]

$$c[l] = \iota[l] \star \iota[-l]. \tag{2}$$

The coarray is non-zero from $l = -(L-1)$ to $l = L-1$, i.e. the support set of the coarray is $-(L-1)$ to $L-1$. We represent the coarray indicator function by $\kappa[l]$. The value of $\kappa[l]$ is 1 if $c[l]$ is non-zero and the value of $\kappa[l]$ is 0 if $c[l]$ is zero. For an L-sensor full array $\kappa[l]$ is 1 for $l = -(L-1)$ to $l = L-1$. However, for sparse arrays, some values of $\kappa[l]$ may be zero. We refer to the array that has $\kappa[l]$ as its sensor location indicator function as a *virtual array* [18]. Sparse arrays whose virtual arrays do not have any missing sensors are called fully augmentable

arrays [16, 31]. Sparse arrays whose virtual arrays have missing sensors are called partially augmentable arrays.

The k^{th} snapshot received by an array with aperture $(L-1)\lambda/2$ is modeled as

$$\mathbf{x}_k = \left(\sum_{d=1}^{\mu} \mathbf{v}(u_d) f_{d,k} + \mathbf{n}_k \right) \odot \boldsymbol{\iota}, \tag{3}$$

where the $L \times 1$ vector $\mathbf{n}_k \sim \mathcal{CN}(0, \sigma_n^2 \mathbf{I})$ represents the noise, μ is the number of plane waves impinging on the array, $f_{d,k} \sim \mathcal{CN}(0, \sigma_d^2)$ is the complex amplitude of the d^{th} plane wave for snapshot k, $u_d = \cos(\theta_d)$ is the direction cosine corresponding to the d^{th} plane wave, θ_d is the angle made by the d^{th} plane wave with the array axis, and $\mathbf{v}(u_d)$ is the steering vectors associated with direction cosine u_d and it is given by [1]

$$\mathbf{v}(u_d) = \begin{bmatrix} e^{0\pi u_d} & e^{1\pi u_d} & \dots & e^{(L-1)\pi u_d} \end{bmatrix}^T. \tag{4}$$

Fig. 1 depicts a scenario where there are $\mu = 2$ plane waves impinging on the array with angles θ_1 and θ_2, respectively. The received signal vector $\mathbf{x}_k$ can also be written as

$$\mathbf{x}_k = \left(\mathbf{V}\mathbf{f}_k + \mathbf{n}_k \right) \odot \boldsymbol{\iota}, \tag{5}$$

where $\mathbf{V} = \begin{bmatrix} \mathbf{v}(u_1) & \mathbf{v}(u_2) & \dots & \mathbf{v}(u_\mu) \end{bmatrix}$ is the array manifold matrix and $\mathbf{f}_k = \begin{bmatrix} f_{1,k} & f_{2,k} & \dots & f_{\mu,k} \end{bmatrix}^T$.

The ensemble covariance matrix of a snapshot is

$$\mathbf{R} = E\{\mathbf{x}_k \mathbf{x}_k^H\}. \tag{6}$$

For a wide-sense stationary (WSS) signal, $\mathbf{R}$ is a Toeplitz matrix. The top panel of Fig. 2 illustrates a full array with 9 sensors and the corresponding virtual array. The virtual array sensors are indicated with unfilled circles. The bottom panel of Fig. 2 depicts the corresponding covariance matrix $\mathbf{R}$. The element $r[l]$ in

the covariance matrix represents the signal autocorrelation function at lag l, i.e. $r[l] = E\{x^*[k]x[k+l]\}$.

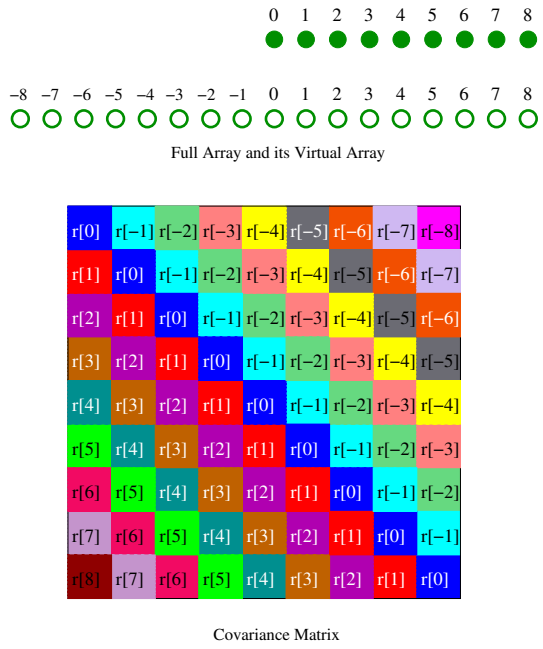

Figure 2. Top: A 9-sensor full ULA and the corresponding virtual array. Bottom: The covariance matrix that can be estimated using the data collected by the full array.

1.3.1 Covariance Matrix Estimation

The ensemble covariance matrix is, in general, not available and needs to be estimated from the array measurements. When K independent snapshots are available, the $L \times K$ data matrix is given by

$$\mathbf{X} = \begin{bmatrix} \mathbf{x}_1 & \mathbf{x}_2 & \dots & \mathbf{x}_K \end{bmatrix}. \tag{7}$$

The $L \times L$ sample covariance matrix corresponding to data matrix $\mathbf{X}$ is

$$\hat{\mathbf{R}} = \mathbf{X}\mathbf{X}^H/K. \tag{8}$$

The sample covariance matrix is the maximum likelihood estimate of the ensemble covariance matrix [1]. Fig. 2 depicts a 9-sensor full ULA and the corresponding

virtual array. The physical sensors are indicated by filled green circles whereas the virtual sensors are indicted by unfilled green circles.

For a sparse array, $\hat{\mathbf{R}}$ contains all-zero columns and rows based on where sensors are missing. In fully augmentable sparse arrays, assuming the received signals are WSS, the $L \times L$ covariance matrix estimate can be obtained from $\hat{\mathbf{R}}$ with diagonal averaging. Diagonal-averaging in fully augmentable arrays replaces any zero element in $\hat{\mathbf{R}}$ by the average of all elements along the diagonal in which the zero element resides. The top panel of Fig. 3 illustrates a fully augmentable sparse array and its virtual array. The bottom panel shows the covariance matrix that can be estimated from the data collected by the sparse array. In partially augmentable sparse arrays, all elements along one or more diagonals of the sample covariance matrix might be zero. Thus, an $L \times L$ covariance matrix estimate cannot be obtained with diagonal averaging in such arrays. The top panel of Fig. 4 shows a partially augmentable array and its virtual array. The unfilled green circles represent virtual sensors whereas the unfilled black circles represent missing virtual sensors. If the hole-free virtual array ranges from $-(H-1)$ to $H-1$, the covariance matrix that can be estimated with the sparse array has size $H \times H$ and $H < L$. For partially augmentable arrays, the right $L-H$ columns and the bottom $L-H$ rows of $\hat{\mathbf{R}}$ are removed before diagonal averaging. As an example, the bottom panel of Fig. 4 depicts the 7×7 covariance matrix that can be estimated for the partially augmentable array in the figure. We denote the covariance matrix estimate corresponding to a sparse array by $\tilde{\mathbf{R}}$.

1.4 Optimal Sensor Locations

For an unbiased estimator, the CRB provides a lower bound on the MSE [30]. For a given aperture and the number of sensors, this section considers finding the sensor locations that correspond to the minimum CRB.

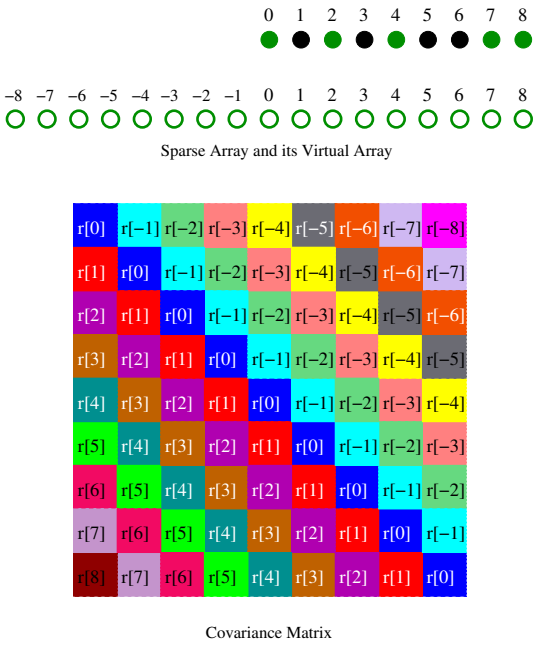

Figure 3. Top: A fully augmentable sparse array and the corresponding virtual array. Bottom: The covariance matrix that can be estimated using the data collected by the sparse array.

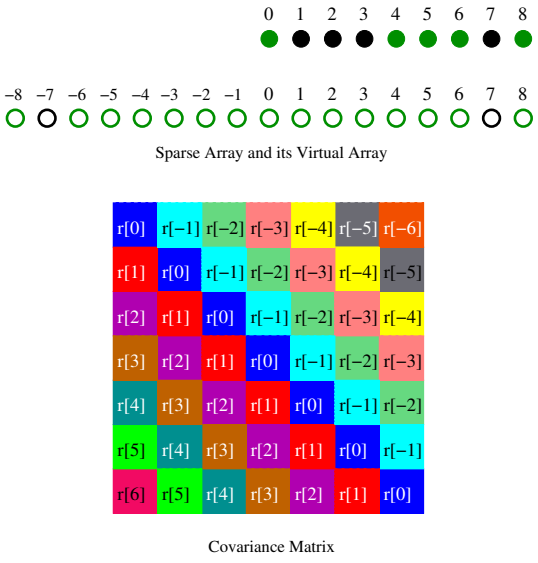

Figure 4. Top: A partially augmentable sparse array and the corresponding virtual array. Bottom: The covariance matrix that can be estimated using the data collected by the sparse array.

We utilize the compact data matrix obtained by removing the all-zero rows from $\mathbf{X}$. We denote the compact data matrix by $\mathbf{Y}$. For a full array, $\mathbf{Y} = \mathbf{X}$ but

not for a sparse array. The size of $\mathbf{Y}$ is $\mathcal{L} \times K$. Note that $\mathcal{L}$ is the number of sensors. For full arrays $\mathcal{L} = L$ whereas for sparse arrays $\mathcal{L} < L$. The ensemble covariance matrix for both full and sparse arrays can be written as $\mathbf{R} = E\{\mathbf{Y}\mathbf{Y}^H\}$. When the signals and noise are uncorrelated and the noise is white, we have

$$\mathbf{R} = \mathbf{V}\mathbf{R}_s\mathbf{V}^H + \sigma_n^2\mathbf{I}_{\mathcal{L}}, \tag{9}$$

where $\mathbf{R}_s = E\{\mathbf{f}_k\mathbf{f}_k^H\}$ is the signal covariance matrix. The $\mu \times \mu$ CRB matrix for DOA estimation is [1]

$$\mathbf{C} = \frac{\sigma_n^2}{2\,\kappa}\left\{\mathrm{Re}\Big\{[\mathbf{R}_s\mathbf{V}^H\mathbf{R}^{-1}\mathbf{V}\mathbf{R}_s] \odot [\mathbf{D}^H\mathbf{P}_{\mathbf{V}}^{\perp}\mathbf{D}]^T\Big\}\right\}^{-1}, \tag{10}$$

where $\mathbf{P}_{\mathbf{V}}^{\perp}$ is the projection matrix onto the noise subspace given by $\mathbf{P}_{\mathbf{V}}^{\perp} = \mathbf{I}_{\mathcal{L}} - \mathbf{V}(\mathbf{V}^H\mathbf{V})^{-1}\mathbf{V}^H$. The matrix $\mathbf{D}$ is the derivative matrix defined as

$$\mathbf{D} = \left[\left.\frac{\partial \mathbf{v}(u)}{\partial u}\right|_{u=u_1}, \left.\frac{\partial \mathbf{v}(u)}{\partial u}\right|_{u=u_2}, \ldots, \left.\frac{\partial \mathbf{v}(u)}{\partial u}\right|_{u=u_\mu}\right].$$

For the single signal case, the Fisher information is

$$\mathbf{J} = \frac{2\,\kappa\,\mathcal{L}\,\eta^2}{(1+\mathcal{L}\,\eta)}\mathbf{d}^H(u_1)\left(1 - \frac{\mathbf{v}(u_1)\mathbf{v}^H(u_1)}{\mathcal{L}}\right)\mathbf{d}(u_1). \tag{11}$$

If $\mathcal{L}$ is odd, the manifold vector $\mathbf{v}(u_1)$ can be expressed as $\mathbf{v}(u_1) = \mathbf{v}_c(u_1)\exp(j\pi 0.5(\mathcal{L}-1))$, where the conjugate symmetric vector

$$\mathbf{v}_c(u_1) = \begin{bmatrix} \exp(j\pi[-0.5(\mathcal{L}-1)]) \\ \exp(j\pi[-0.5(\mathcal{L}-1)+1]) \\ \vdots \\ \exp(j\pi[0.5(\mathcal{L}-1)-1]) \\ \exp(j\pi 0.5(\mathcal{L}-1)) \end{bmatrix} \tag{12}$$

is the array manifold vector of an $\mathcal{L}$-element ULA whose phase center is at the origin. The vector $\mathbf{d}(u_1)$ can be expressed as

$$\mathbf{d}(u_1) = \exp(j\pi 0.5(\mathcal{L}-1))[\mathbf{d}_c(u_1) + \mathbf{v}_c(u_1)j\pi 0.5(\mathcal{L}-1)], \tag{13}$$

where $\mathbf{d}_c(u_1) = \partial \mathbf{v}_c(u)/\partial u|_{u=u_1}$. The term that is dependent on the sensor locations in (11) is

$$\begin{aligned} J_1 &= \mathbf{d}^H(u_1)\left(1 - \frac{\mathbf{v}(u_1)\mathbf{v}^H(u_1)}{\mathcal{L}}\right)\mathbf{d}(u_1) \\ &= ||\mathbf{d}(u_1)||^2 - |\mathbf{d}^H(u_1)\mathbf{v}(u_1)|^2. \end{aligned} \tag{14}$$

Since $||\mathbf{d}(u_1)||^2 = ||\mathbf{d}_c(u_1)||^2 + 0.25\pi^2\,\mathcal{L}(\mathcal{L}-1)^2$ and $\mathbf{d}^H(u_1)\mathbf{v}(u_1) = -0.5j\pi\,\mathcal{L}(\mathcal{L}-1)$, the only term in (14) that is dependent on the sensor locations is

$$J_2 = ||\mathbf{d}_c(u_1)||^2. \tag{15}$$

Thus, minimization of the CRB is equivalent to the maximization of J_2, which is the sum of the squares of the elements of the following vector

$$\pi \begin{bmatrix} -(\mathcal{L}-1)/2 \\ -(\mathcal{L}-1)/2+1 \\ \cdots \\ (\mathcal{L}-1)/2-1 \\ (\mathcal{L}-1)/2 \end{bmatrix} = \pi\mathbf{i}, \tag{16}$$

where $\mathbf{i}$ is the index vector. To maximize $||\pi\mathbf{i}||^2$ while choosing only M sensors, the top half and bottom half elements of $\mathbf{i}$ should be chosen. If M is odd, we can either pick $(M-1)/2$ top indices and $(M+1)/2$ bottom indices or $(M-1)/2$ bottom indices and $(M+1)/2$ top indices. An analogous derivation and thus conclusion follow if $\mathcal{L}$ is even. To verify this optimal selection algorithm, we consider an array with $\mathcal{L} = 15$ and $M = 10$. We found the CRB corresponding to each 10-sensor sparse array. There are 3003 possible sparse arrays. The CRBs are plotted in Fig. 5. The minimum CRB value is also indicated in the figure. The sensor combination number corresponding to the minimum CRB is 252, which is associated with $\boldsymbol{\iota} = [1,1,1,1,1,0,0,0,0,0,1,1,1,1,1]$.

When the number of plane waves impinging on the array is more than 1, the sparse array that minimizes the CRB cannot be found analytically.

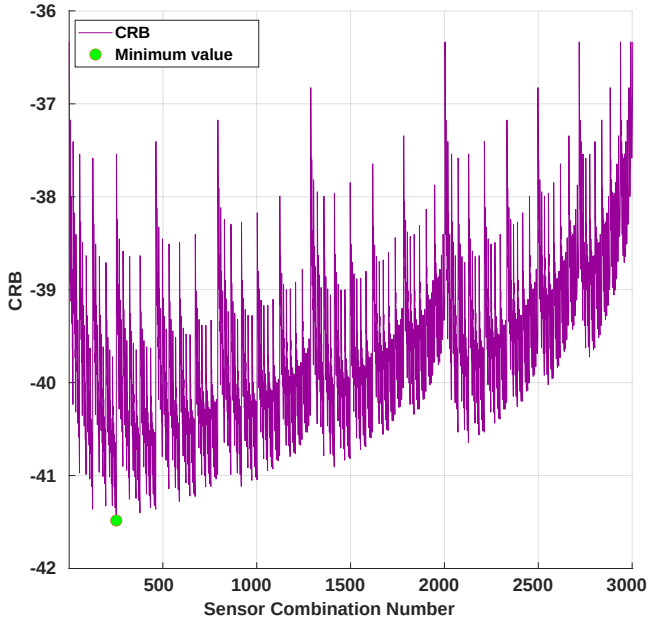

Figure 5. The CRB values for 3003 different sparse arrays. The total number of sensors in the full array is $\mathcal{L} = 15$. The total number of sensors in each sparse array is $\mathcal{L} = 10$.

1.5 Analysis of MSE for Full and Sparse Arrays

This section analyzes the MSEs in DOA estimation using full and sparse arrays. We consider the two prominent subspace-based DOA estimation algorithms: MUSIC and MNM.

The first example analyzes the trade-offs in using the sample covariance matrix $\hat{\mathbf{R}}$ and the diagonal-averaged covariance matrix $\tilde{\mathbf{R}}$ for a full ULA. We consider a scenario where $\mathcal{L} = 12$ and there are two closely located sources with direction cosines $u_1 = -0.5\Delta u$ and $u_2 = 0.5\Delta u$, where $\Delta u = 0.2165 \times 4/\mathcal{L}$ is the half-power beamwidth of the array. For each value of SNR, we evaluated MSEs for MUSIC and MNM using 500 independent trials. The top panel of Fig. 6 plots the MSEs for different values of SNR. When SNR is low (less than -20 dB in the figure), the MSEs for both MUSIC and MNM are constant. [1] notes that in this region the DOA estimates have a uniform distribution, i.e. $u_i \sim \mathcal{U}(-1, 1)$. When the

SNR increases to -10 dB, the MSEs for both algorithms begin to descend and become approximately equal to the CRB. The SNR at which the MSE becomes approximately equal to the CRB is called threshold SNR and the region below the threshold SNR is called subspace-swap region [32, 33]. The threshold SNR in Fig. 6 is 4 dB. When the SNR further increases to 37 dB, the MSEs deviate from the CRB again. Note that [1] analyzes these MSEs only up to SNR of 20 dB and assumes incorrectly that the MSEs follow the CRB for higher values of SNR. The bottom panel of Fig. 6 plots the bias-squared and variance for both algorithms. The MSE is equal to the sum of bias-squared and variance [30]. The figure depicts the trade-offs between bias and variance. When the SNR is below the threshold SNR, the bias and variance are commensurate. In the region where the SNR is above the threshold SNR and the MSEs are close to the CRB, the biases are negligible compared to the variances. Consequently, the MSEs are almost equal to the respective variances. At very high SNR, when the MSEs deviate from the CRB, the variances are negligible compared to the biases. Thus, the MSEs in this region are contributed almost entirely by the biases.

Fig. 7 plots the MSEs, biases, and variances for the 12-sensor full ULA using $\tilde{\mathbf{R}}$ with the MUSIC and MNM algorithms. The threshold SNR is for the two algorithms is -2 dB. Thus, the subspace-swap region is shorter and ends at a lower value of SNR compared to Fig. 6. However, the MSEs start deviating from the CRB at only 10 dB. Thus, for SNR less than 10 dB, the MUSIC and MNM algorithms are more accurate with $\tilde{\mathbf{R}}$. For SNR higher than 10 dB, the algorithms are more accurate with $\hat{\mathbf{R}}$. The comparison between the bias and variances in the bottom panel of Fig. 7 illustrates that below the threshold SNR, the bias and variances are comparable. The bias is almost negligible and the MSE is approximately equal to the variances when the SNR is higher than the threshold SNR.

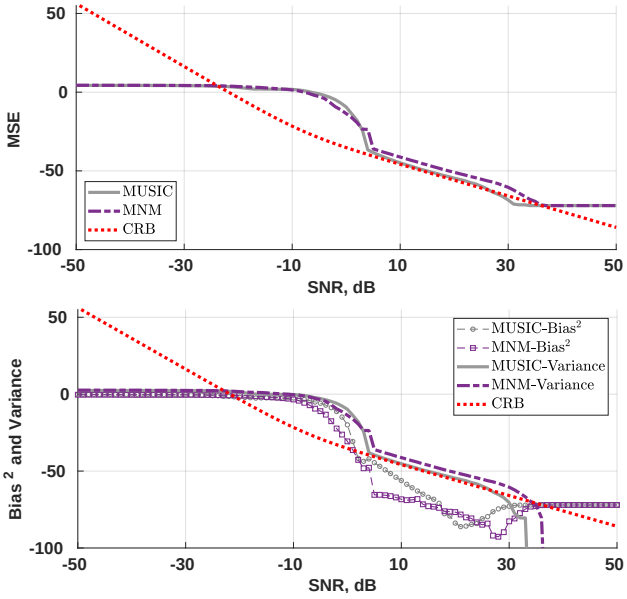

Figure 6. Performance analysis of MUSIC and MNM for a 12-sensor full ULA using $\hat{\mathbf{R}}$. Top: MSEs. Bottom: Bias and Variance.

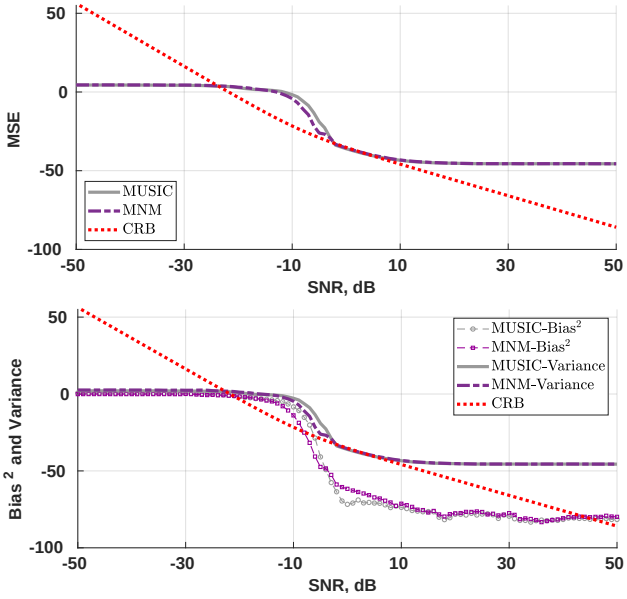

Figure 7. Performance analysis of MUSIC and MNM for a 12-sensor full ULA using $\tilde{\mathbf{R}}$. Top: MSEs. Bottom: Bias and Variance.

Fig. 8 plots the MSEs for a fully augmentable sparse array with 10 sensors. The sensor location indicator vector is $\boldsymbol{\kappa} = [1, 1, 1, 1, 0, 0, 1, 1, 1, 1, 1]$. The MSE

trends in Fig. 8 and Fig. 7 are similar. The threshold SNR is 0 dB and the high SNR value at which the MSEs deviate from the CRB is 8 dB. Compared to Fig. 7, the SNR range over which the MSEs are close to the CRB is narrower, which can be attributed to the decrease in the number of sensors.

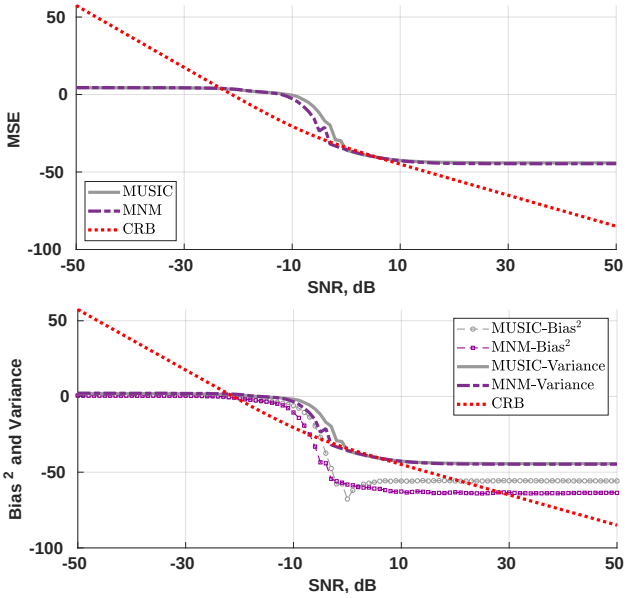

Figure 8. Performance analysis of MUSIC and MNM for a 10-sensor sparse array using $\tilde{\mathbf{R}}$. Top: MSEs. Bottom: Bias and Variance.

The array gain or detection gain of a ULA for white noise is equal to the number of sensors [1]. For sparse arrays, the detection gain is approximately linear with the number of sensors [34, 35]. To examine if the MSE and CRB are linear with the number of sensors for a linear array with a fixed aperture, we consider an array with $30\lambda/2$ aperture. Fig. 9 plots the MSEs and CRBs for the array with increasing sparsity. The sensor locations are depicted in the top panel of Fig. 9. The fixed sensors are indicated by green circles while the removable sensors are indicated by red squares. Since the sensors numbered 20, 30, and 0 to 10 are kept fixed, the array is always fully augmentable. The removable sensors are discarded one at a time, starting from the right end and moving towards left.

The middle panel plots the MUSIC MSEs and CRBs at fixed SNR with increasing sparsity. SNR values of 0 dB (purple dash-dot line) and 10 dB (blue dash line) are considered. The CRBs and MSEs do not vary linearly with the number of sensors. Similarly, the bottom panel plots the MNM MSEs and CRBs. For this case also, the CRBs and MSEs do not exhibit linear dependence on the number of sensors.

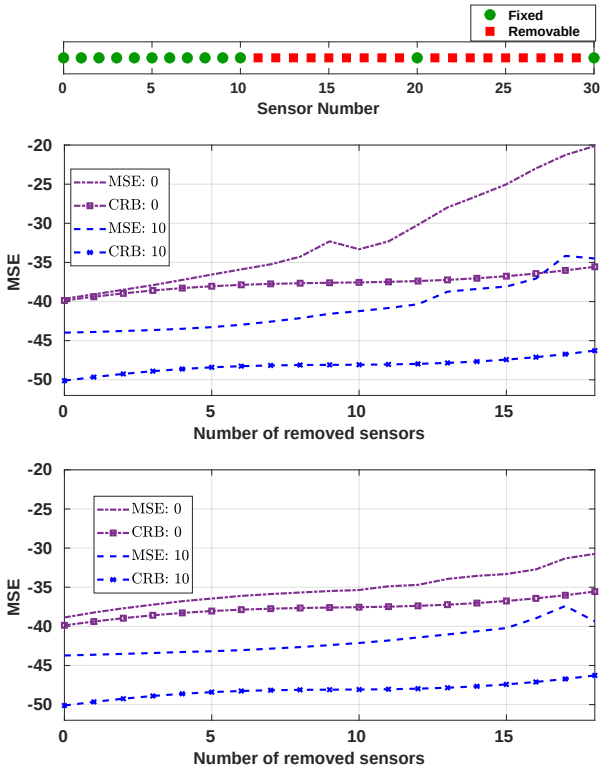

Figure 9. Variation of MSE and CRB with the array sparsity. The SNR values are 0 dB (purple dash-dot line) and 10 dB (blue dash line). Top: Sensor locations. Middle: MUSIC. Bottom: MNM.

1.6 Conclusion

For a given number of sensors and aperture, we derived an analytical technique to select M sensors out of $\mathcal{L}$ sensors while minimizing the CRB. The result is valid for the single plane wave case. We verified the result using a combinatorial search for selecting 10 sensors out of 15 sensors. For a full array, we compared MSEs,

biases, and variances of MUSIC and MNM algorithms using sample covariance matrix and diagonal-averaged covariance matrix. The MSE trends when using the two different covariance estimates were observed to be similar. The MSE patterns of a fully augmentable sparse array for the MUSIC and MNM alogrithms were similar to the full array case using the diagonal-averaged covariance matrix. However, as expected, the MSEs were higher for a sparse array than for a full array with an equal aperture due the reduction in the number of sensors. The analysis of the MUSIC and MNM MSEs for a sparse array revealed non-linear dependence on the number of sensors.

List of References

[1] H. Van Trees, *Optimum Array Processing (Detection, Estimation and Modulation Theory, Part IV)*. John Wiley and Sons, Inc., New York, 2002.

[2] D. Johnson and D. Dudgeon, *Array Signal Processing: Concepts and Techniques*. Simon & Schuster, 1992.

[3] K. Adhikari, J. Buck, and K. Wage, "Extending coprime sensor arrays to achieve the peak side lobe height of a full uniform linear array," *EURASIP Journal on Advances in Signal Processing*, vol. 2014, no. 1, p. 148, Sep 2014. [Online]. Available: https://doi.org/10.1186/1687-6180-2014-148

[4] K. Adhikari, J. Buck, and K. Wage, "Beamforming with extended co-prime sensor arrays," *2013 IEEE International Conference on Acoustics, Speech and Signal Processing (ICASSP)*, pp. 4183–4186, May 2013.

[5] K. Adhikari and B. Drozdenko, "Design and statistical analysis of tapered coprime and nested arrays for the min processor," *IEEE Access*, vol. 7, pp. 139 601–139 615, 2019.

[6] P. Vaidyanathan and P. Pal, "Sparse sensing with co-prime samplers and arrays," *IEEE Transactions on Signal Processing*, vol. 59, no. 2, pp. 573–586, February 2011.

[7] P. Pal and P. Vaidyanathan, "Nested arrays: A novel approach to array processing with enhanced degrees of freedom," *IEEE Transactions on Signal Processing*, vol. 58, no. 8, pp. 4167 –4181, August 2010.

[8] K. Adhikari and J. Buck, "Spatial spectral estimation with product processing of a pair of colinear arrays," *IEEE Transactions on Signal Processing*, vol. 65, no. 9, pp. 2389–2401, May 2017.

[9] K. Wage, "When two wrongs make a right: Combining aliased arrays to find sound sources," *Acoustics Today*, vol. 14, no. 3, pp. 48–56, 2018.

[10] K. Adhikari, B. M. Harker, T. A. Wettergren, L. A. Freeman, and S. E. Freeman, "Array shading to maximize deflection coefficient for broadband signal detection with conventional beamforming," *IEEE Access*, vol. 9, pp. 79 343–79 352, 2021.

[11] D. Sartori and K. Adhikari, "Product processing for tapered sparse arrays," in *2021 International Conference on Electrical, Communication, and Computer Engineering (ICECCE)*, 2021, pp. 1–6.

[12] K. Adhikari, "Beamforming with semi-coprime arrays," *The Journal of the Acoustical Society of America*, vol. 145, no. 5, pp. 2841–2850, 2019. [Online]. Available: https://doi.org/10.1121/1.5100281

[13] K. Adhikari and B. Drozdenko, "Symmetry-imposed rectangular coprime and nested arrays for direction of arrival estimation with multiple signal classification," *IEEE Access*, vol. 7, pp. 153 217–153 229, 2019.

[14] S. Pillai and F. Haber, "Statistical analysis of a high resolution spatial spectrum estimator utilizing an augmented covariance matrix," *IEEE Transactions on Acoustics, Speech and Signal Processing*, vol. 35, no. 11, pp. 1517–1523, November 1987.

[15] K. Adhikari and T. Trosclair, "Minimum norm method for linear and planar sparse arrays," in *2021 International Conference on Electrical, Communication, and Computer Engineering (ICECCE)*, 2021, pp. 1–6.

[16] Y. I. Abramovich, D. A. Gray, A. Y. Gorokhov, and N. K. Spencer, "Positive-definite toeplitz completion in doa estimation for nonuniform linear antenna arrays. i. fully augmentable arrays," *IEEE Transactions on Signal Processing*, vol. 46, no. 9, pp. 2458–2471, 1998.

[17] Y. Abramovich, N. Spencer, and A. Gorokhov, "Detection-estimation of more uncorrelated gaussian sources than sensors in nonuniform linear antenna arrays. ii. partially augmentable arrays," *IEEE Transactions on Signal Processing*, vol. 51, no. 6, pp. 1492–1507, 2003.

[18] K. Adhikari and B. Drozdenko, "Comparison of music variants for sparse arrays," *2019 IEEE National Aerospace and Electronics Conference (NAECON)*, pp. 398–405, 2019.

[19] K. Adhikari, R. J. Vaccaro, and D. D. Sartori, "Shift invariant sparse arrays and their optimal signal and noise subspaces," *Signal Processing*, vol. 198, p. 108579, 2022. [Online]. Available: https://www.sciencedirect.com/science/article/pii/S0165168422001207

[20] R. Schmidt, "Multiple emitter location and signal parameter estimation," *IEEE Transactions on Antennas and Propagation*, vol. 34, no. 3, pp. 276–280, March 1986.

[21] R. Kumaresan and D. W. Tufts, "Estimating the angles of arrival of multiple plane waves," *IEEE Transactions on Aerospace and Electronic Systems*, vol. AES-19, no. 1, pp. 134–139, Jan 1983.

[22] A. Maffett, "Array factors with nonuniform spacing parameter," *IRE Transactions on Antennas and Propagation*, vol. 10, no. 2, pp. 131–136, 1962.

[23] A. Moffet, "Minimum-redundancy linear arrays," *IRE Trans. Antennas Propag.*, vol. 16, pp. 172–175, March 1968.

[24] D. Davies and C. Ward, "Low sidelobe patterns from thinned arrays using multiplicative processing," *IEE Proceedings F Communications, Radar and Signal Processing*, vol. 127, no. 1, pp. 9–23, February 1980.

[25] S. Mitra, K. Mondal, M. Tchobanou, and G. Dolecek, "General polynomial factorization-based design of sparse periodic linear arrays," *IEEE Transactions on Ultrasonics, Ferroelectrics, and Frequency Control*, vol. 57, no. 9, pp. 1952–1966, September 2010.

[26] D. King, R. Packard, and R. Thomas, "Unequally-spaced, broad-band antenna arrays," *IRE Transactions on Antennas and Propagation*, vol. 8, no. 4, pp. 380–384, 1960.

[27] B. P. Kumar and G. R. Branner, "Design of unequally spaced arrays for performance improvement," *IEEE Transactions on Antennas and Propagation*, vol. 47, no. 3, pp. 511–523, 1999.

[28] K. Adhikari and S. Kay, "Optimal sparse sampling for detection of a known signal in nonwhite gaussian noise," *IEEE Signal Processing Letters*, pp. 1–1, 2021.

[29] S. Kay and S. Saha, "Design of sparse linear arrays by monte carlo importance sampling," *IEEE Journal of Oceanic Engineering*, vol. 27, no. 4, pp. 790–799, 2002.

[30] S. Kay, *Fundamentals of Statistical Signal Processing: Estimation Theory, Vol. I.* Prentice Hall, Englewood Cliffs, NJ, 1993.

[31] K. Adhikari, "Absolute eigenvalues-based covariance matrix estimation for a sparse array," in *2021 IEEE Statistical Signal Processing Workshop (SSP)*, 2021, pp. 401–405.

[32] D. Tufts, A. Kot., and R. Vaccaro, "The threshold effect in signal processing algorithms which use an estimated subspace," *SVD and Signal Processing II: Algorithms, Analysis and Applications Ed. New York: Elsevier*, 1991.

[33] J. Thomas, L. Scharf, and D. Tufts, "The probability of a subspace swap in the svd," *IEEE Transactions on Signal Processing*, vol. 43, no. 3, pp. 730–736, 1995.

[34] K. Adhikari and J. Buck, "Gaussian signal detection by coprime sensor arrays," *2015 IEEE International Conference on Acoustics, Speech and Signal Processing (ICASSP)*, pp. 2379–2383, April 2015.

[35] K. Adhikari and J. Buck, "Gaussian signal detection with product arrays," *IEEE Access*, vol. 7, pp. 36 256–36 266, 2020.

BIBLIOGRAPHY

Abramovich, Y. I., Gray, D. A., Gorokhov, A. Y., and Spencer, N. K., "Positive-definite toeplitz completion in doa estimation for nonuniform linear antenna arrays. i. fully augmentable arrays," *IEEE Transactions on Signal Processing*, vol. 46, no. 9, pp. 2458–2471, 1998.

Abramovich, Y., Spencer, N., and Gorokhov, A., "Detection-estimation of more uncorrelated gaussian sources than sensors in nonuniform linear antenna arrays. ii. partially augmentable arrays," *IEEE Transactions on Signal Processing*, vol. 51, no. 6, pp. 1492–1507, 2003.

Adhikari, K., "Beamforming with semi-coprime arrays," *The Journal of the Acoustical Society of America*, vol. 145, no. 5, pp. 2841–2850, 2019. [Online]. Available: https://doi.org/10.1121/1.5100281

Adhikari, K. and Buck, J., "Gaussian signal detection by coprime sensor arrays," *2015 IEEE International Conference on Acoustics, Speech and Signal Processing (ICASSP)*, pp. 2379–2383, April 2015.

Adhikari, K. and Buck, J., "Spatial spectral estimation with product processing of a pair of colinear arrays," *IEEE Transactions on Signal Processing*, vol. 65, no. 9, pp. 2389–2401, May 2017.

Adhikari, K. and Buck, J., "Gaussian signal detection with product arrays," *IEEE Access*, vol. 7, pp. 36 256–36 266, 2020.

Adhikari, K., Buck, J., and Wage, K., "Beamforming with extended co-prime sensor arrays," *2013 IEEE International Conference on Acoustics, Speech and Signal Processing (ICASSP)*, pp. 4183–4186, May 2013.

Adhikari, K., Buck, J., and Wage, K., "Extending coprime sensor arrays to achieve the peak side lobe height of a full uniform linear array," *EURASIP Journal on Advances in Signal Processing*, vol. 2014, no. 1, p. 148, Sep 2014. [Online]. Available: https://doi.org/10.1186/1687-6180-2014-148

Adhikari, K. and Drozdenko, B., "Comparison of music variants for sparse arrays," *2019 IEEE National Aerospace and Electronics Conference (NAECON)*, pp. 398–405, 2019.

Adhikari, K. and Drozdenko, B., "Design and statistical analysis of tapered coprime and nested arrays for the min processor," *IEEE Access*, vol. 7, pp. 139 601–139 615, 2019.

Adhikari, K. and Drozdenko, B., "Symmetry-imposed rectangular coprime and nested arrays for direction of arrival estimation with multiple signal classification," *IEEE Access*, vol. 7, pp. 153 217–153 229, 2019.

Adhikari, K., "Absolute eigenvalues-based covariance matrix estimation for a sparse array," in *2021 IEEE Statistical Signal Processing Workshop (SSP)*, 2021, pp. 401–405.

Adhikari, K., Harker, B. M., Wettergren, T. A., Freeman, L. A., and Freeman, S. E., "Array shading to maximize deflection coefficient for broadband signal detection with conventional beamforming," *IEEE Access*, vol. 9, pp. 79 343–79 352, 2021.

Adhikari, K. and Kay, S., "Optimal sparse sampling for detection of a known signal in nonwhite gaussian noise," *IEEE Signal Processing Letters*, pp. 1–1, 2021.

Adhikari, K. and Trosclair, T., "Minimum norm method for linear and planar sparse arrays," in *2021 International Conference on Electrical, Communication, and Computer Engineering (ICECCE)*, 2021, pp. 1–6.

Adhikari, K., Vaccaro, R. J., and Sartori, D. D., "Shift invariant sparse arrays and their optimal signal and noise subspaces," *Signal Processing*, vol. 198, p. 108579, 2022. [Online]. Available: https://www.sciencedirect.com/science/article/pii/S0165168422001207

Davies, D. and Ward, C., "Low sidelobe patterns from thinned arrays using multiplicative processing," *IEE Proceedings F Communications, Radar and Signal Processing*, vol. 127, no. 1, pp. 9–23, February 1980.

Johnson, D. and Dudgeon, D., *Array Signal Processing: Concepts and Techniques*. Simon & Schuster, 1992.

Kay, S. and Saha, S., "Design of sparse linear arrays by monte carlo importance sampling," *IEEE Journal of Oceanic Engineering*, vol. 27, no. 4, pp. 790–799, 2002.

Kay, S., *Fundamentals of Statistical Signal Processing: Estimation Theory, Vol. I*. Prentice Hall, Englewood Cliffs, NJ, 1993.

King, D., Packard, R., and Thomas, R., "Unequally-spaced, broad-band antenna arrays," *IRE Transactions on Antennas and Propagation*, vol. 8, no. 4, pp. 380–384, 1960.

Kumar, B. P. and Branner, G. R., "Design of unequally spaced arrays for performance improvement," *IEEE Transactions on Antennas and Propagation*, vol. 47, no. 3, pp. 511–523, 1999.

Kumaresan, R. and Tufts, D. W., "Estimating the angles of arrival of multiple plane waves," *IEEE Transactions on Aerospace and Electronic Systems*, vol. AES-19, no. 1, pp. 134–139, Jan 1983.

Maffett, A., "Array factors with nonuniform spacing parameter," *IRE Transactions on Antennas and Propagation*, vol. 10, no. 2, pp. 131–136, 1962.

Mitra, S., Mondal, K., Tchobanou, M., and Dolecek, G., "General polynomial factorization-based design of sparse periodic linear arrays," *IEEE Transactions on Ultrasonics, Ferroelectrics, and Frequency Control*, vol. 57, no. 9, pp. 1952–1966, September 2010.

Moffet, A., "Minimum-redundancy linear arrays," *IRE Trans. Antennas Propag.*, vol. 16, pp. 172–175, March 1968.

Pal, P. and Vaidyanathan, P., "Nested arrays: A novel approach to array processing with enhanced degrees of freedom," *IEEE Transactions on Signal Processing*, vol. 58, no. 8, pp. 4167 –4181, August 2010.

Pillai, S. and Haber, F., "Statistical analysis of a high resolution spatial spectrum estimator utilizing an augmented covariance matrix," *IEEE Transactions on Acoustics, Speech and Signal Processing*, vol. 35, no. 11, pp. 1517–1523, November 1987.

Sartori, D. and Adhikari, K., "Product processing for tapered sparse arrays," in *2021 International Conference on Electrical, Communication, and Computer Engineering (ICECCE)*, 2021, pp. 1–6.

Schmidt, R., "Multiple emitter location and signal parameter estimation," *IEEE Transactions on Antennas and Propagation*, vol. 34, no. 3, pp. 276–280, March 1986.

Thomas, J., Scharf, L., and Tufts, D., "The probability of a subspace swap in the svd," *IEEE Transactions on Signal Processing*, vol. 43, no. 3, pp. 730–736, 1995.

Tufts, D., Kot., A., and Vaccaro, R., "The threshold effect in signal processing algorithms which use an estimated subspace," *SVD and Signal Processing II: Algorithms, Analysis and Applications Ed. New York: Elsevier*, 1991.

Vaidyanathan, P. and Pal, P., "Sparse sensing with co-prime samplers and arrays," *IEEE Transactions on Signal Processing*, vol. 59, no. 2, pp. 573–586, February 2011.

Van Trees, H., *Optimum Array Processing (Detection, Estimation and Modulation Theory, Part IV)*. John Wiley and Sons, Inc., New York, 2002.

Wage, K., "When two wrongs make a right: Combining aliased arrays to find sound sources," *Acoustics Today*, vol. 14, no. 3, pp. 48–56, 2018.